

BIOFUEL PRODUCTION FROM SOLID AND LIQUID FRACTIONS OF HYDROTHERMALLY PRETREATED SUGARCANE BAGASSE IN A CONTINUOUS COMPARTMENTALIZED REACTOR AND POTENTIAL METABOLIC PATHWAYS

Laís A. Soares^a, Lucas T. Fuess^{a,*},, Tiago P. Delforno^b, Valéria M. Oliveira^c, Edson L. Silva^d and Maria B. A. Varesche^a

^aDepartamento de Hidráulica e Saneamento, Escola de Engenharia de São Carlos, Universidade de São Paulo, 13563-120 São Carlos – SP, Brasil

^bInstituto SENAI de Inovação em Biotecnologia, 01130-000 São Paulo – SP, Brasil

^cDivisão de Recursos Microbianos, Centro Pluridisciplinar de Pesquisas Químicas, Biológicas e Agrícolas, Universidade Estadual de Campinas, 13148-218 Campinas – SP, Brasil

^dDepartamento de Engenharia Química, Universidade Federal de São Carlos, 13565-905 São Carlos – SP, Brasil

Received: 09/21/2023; accepted: 01/24/2024; published online: 03/20/2024

Solid and liquid fractions of hydrothermally pretreated sugarcane bagasse (SCB) were simultaneously used as substrate of a novel continuous compartmentalized reactor. The effect of four (56, 42, 28, and 14 h) hydraulic retention time (HRT) and three (0.5, 3.0, and 9.0 g L⁻¹) chemical oxygen demand (COD) levels were evaluated on hydrogen (H₂) and organic acids production. Higher H₂ production and yield (686 mL and 1.63 mol mol⁻¹ carbohydrate, respectively) were obtained under an HRT of 28 h, probably due to the *Clostridium* and *Thermoanaerobacterium* metabolisms, which accounted for almost 60% of the microbial relative abundance. Under lower and higher HRT (14 and 56 h, respectively) lactic acid prevailed without hydrogen production. Other value-added chemicals such as citric, valeric and caproic acids were also obtained according to the HRT. From the functional point of view, enzymes from the glycoside hydrolases group (GHs) potentially performed important roles in the lignocellulosic biomass bioconversion.

Keywords: biorefinery; building-block chemicals; hydrothermal pretreatment; lignocellulosic biomass; metagenomics analysis.

INTRODUCTION

Sugarcane bagasse (SCB) is one of the most abundantly generated by-products in the Brazilian sucro-alcohol industry, presenting a high potential value for energy production due to its organic-rich nature. The production of biohydrogen and organic acids from the anaerobic processing of lignocellulosic biomass has gained increasing attention because it combines energy generation and waste reduction.

Usually, the bioconversion of lignocellulosic biomass into biofuels comprises pretreatment, enzymatic hydrolysis, and fermentation steps. The pretreatment step is required due to the strong linkage between cellulose, hemicellulose and lignin by covalent and non-covalent bonds forming a complex and recalcitrant lignocellulosic matrix,¹ which results in an obstacle to its biodegradation.

The hydrothermal process is one of the most commonly used pretreatment methods of lignocellulosic biomass. In this pretreatment the fiber is maintained under high pressure and temperature and then quickly depressurized, resulting in a slightly acidic liquid hydrolysate and a solid fraction.

The solid fraction is usually used as substrate to feed batch reactors,² while the liquid is used to feed continuous reactors.³ According to Ribeiro *et al.*,³ the liquid fraction of SCB hydrothermal pretreatment contains mainly xylose, one of the hemicellulose constituents, once it is more hydrolyzed than the affected cellulose during hydrothermal pretreatments, which can be used to produce biogas *via* anaerobic digestion.

As a response of the hydrothermal pretreatment, the cellulose content increases, with the concomitant reduction of lignin and xylan contents due to the partial degradation of xylan releasing xylan oligomers, while the hydrophobic lignin and less reactive cellulose

persist in the fiber¹ and can be used as substrate for energy production *via* fermentation.

Given the complexity of both solid and liquid fractions resulting from hydrothermally pretreated SCB, understanding the microbial interactions in bioreactors is an important aspect to understand the hydrolysis and fermentation steps, in order to improve bioenergy recovery from the lignocellulosic biomass.

Microbial populations in thermophilic acidogenic reactors applied to sugarcane bagasse have already been characterized in recent studies.² *Clostridium* and *Thermoanaerobacterium* are key microorganisms involved in the bioconversion of sugarcane-derived by-products.⁴ *Clostridium* is able to perform hydrolysis of lignocellulosic biomass such as sugarcane bagasse due to the production of cellulase enzymes, such as endoglucanases, cellobiohydrolases and β -glycosidase⁵ grouped into glycoside hydrolases (GHs) family enzymes. In particular, this genus is widely associated to hydrolysis and fermentation steps, resulting in hydrogen production *via* acetic and butyric acid pathways. However, this genus is also able to perform different metabolic pathways resulting in the production of different organic acids.⁶ Taking this into account, this study aimed to develop an innovative reactor able to convert the solid and liquid fractions resulting from the hydrothermal pretreatment of SCB into biohydrogen and value-added soluble metabolites, also using the fibers as support material for microbial adhesion. SCB-derived hydrolysate was used as a source of reducing sugars. Finally, to better understand the microbial pathways and screen the synergetic and functional enzymatic profile, gene functions annotated during the metagenomic analysis which were homologous to those deposited in the carbohydrate active enzymes database (CAZy) were described.

*e-mail: lt.fuess@usp.br

EXPERIMENTAL

Sugarcane bagasse and hydrolysate

SCB hydrothermally pretreated at 200 °C for 10 min, according to Soares *et al.*,² and hydrolysate (190 °C for 10 min) were collected from the Laboratório Nacional de Biorrenováveis (LNBR, Brazilian Biorenewables National Laboratory) located in Campinas, SP, Brazil.

Inoculum

Anaerobic sludge was collected from a thermophilic (55 °C) upflow anaerobic sludge blanket (UASB) reactor applied in the treatment of sugarcane vinasse at the São Martinho distillery plant, located in Pradópolis, SP, Brazil. The sludge was thermally treated (90 °C for 10 min) to stimulate the growth of endospore-forming fermentative bacteria.⁷ The microorganisms selected during the thermal treatment of the sludge were bioaugmented with endogenous communities adhered to raw SCB, previously enriched in batch flasks (10 g L⁻¹) using cellulolytic medium⁸ supplemented with 3 g L⁻¹ of yeast extract.⁹

Operational conditions

Four compartmented anaerobic fixed-bed reactors (0.805 L each) were continuously operated for 238 days at different HRT (R1 - 56 h,

R2 - 42 h, R3 - 28 h, and R4 - 14 h) and thermophilic condition (55 °C). The reactors are formed by six compartments (length-to-diameter, L/D = 0.3, 1.5, 2.7, 3.9, 5.1, and 6.3) separated by five bed-like structures filled with fiber recovered after the hydrothermal pretreatment (200 °C at 16 bar for 10 min) of sugarcane bagasse. The reactors were fed in upflow mode, and the fibers were used simultaneously as support material for microbial adhesion and substrate. Figure 1 shows the reactor design and the main characteristics of the experimental apparatus. This innovative design allows the operation of continuous reactors fed with solid and liquid substrate. The inoculum was recirculated for 17 days for adaptation and adhesion of the microorganisms on the surface of SCB available in the compartments. Peristaltic pumps (Model Minipuls Evolution, Gilson, Inc., Middleton, WI, USA) were used to feed all the reactors with the hydrolysate in four phases according to the chemical oxygen demand (COD) (Table 1).

Analytical methods

COD and pH were evaluated according to the methodologies described in the Standard Methods for the Examination of Water and Wastewater.¹⁰ Organic acids (acetic, propionic, butyric, isobutyric, valeric, isovaleric and caproic acids) and sugars (glucose, sucrose, xylose, galactose and arabinose) were analyzed by high performance liquid chromatography (HPLC) equipped with a UV diode array detector (SPD-M10 AVP), a refraction index detector (RID-10A), a

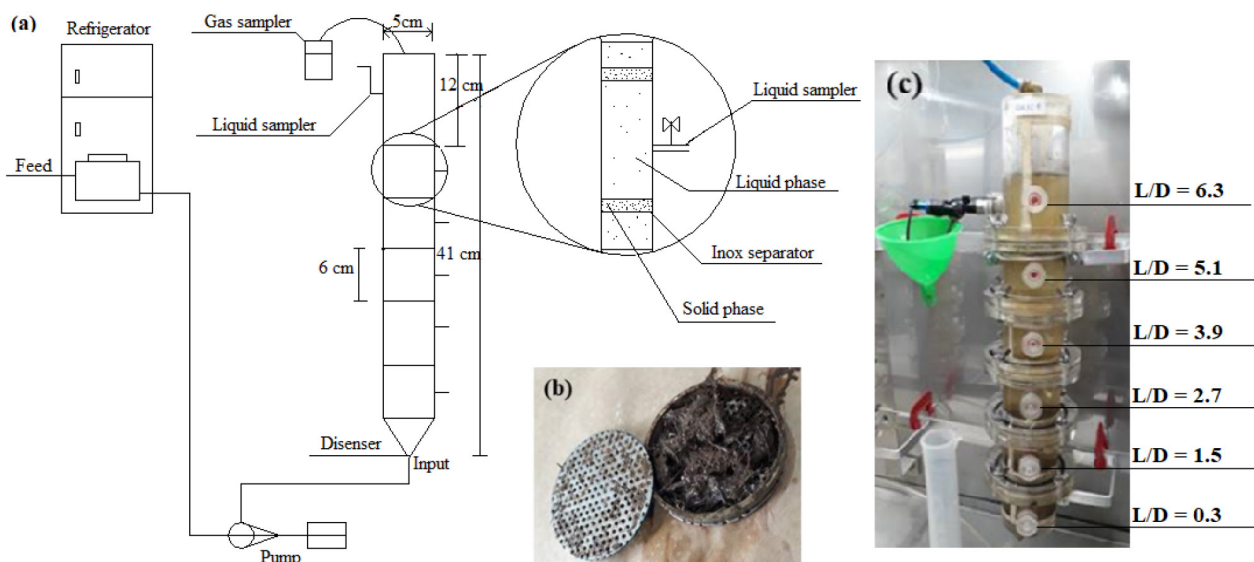


Figure 1. (a) Layout of the experimental apparatus; (b) solid phase compartment; (c) operational system. L (length)/D (diameter)

Table 1. Operating conditions applied in each reactor

| Operating phase | Control parameter | Reactor (HRT / h) | | | |
|-----------------|----------------------------|-----------------------|-----------------------|-----------------------|-----------------------|
| | | R ₁ (56.0) | R ₂ (42.0) | R ₃ (28.0) | R ₄ (14.0) |
| Phase 1 | COD / (g L ⁻¹) | 0.5 ± 0.1 | 0.5 ± 0.1 | 0.5 ± 0.05 | 0.5 ± 0.1 |
| | pH | 5.8 ± 0.3 | 5.8 ± 0.3 | 5.8 ± 0.3 | 5.8 ± 0.3 |
| Phase 2 | COD / (g L ⁻¹) | 3.2 ± 0.4 | 3.2 ± 0.4 | 3.2 ± 0.4 | 3.2 ± 0.4 |
| | pH | 4.3 ± 0.2 | 4.3 ± 0.3 | 4.3 ± 0.2 | 4.3 ± 0.2 |
| Phase 3 | COD / (g L ⁻¹) | 9.2 ± 0.8 | 9.2 ± 0.8 | 9.2 ± 0.8 | 9.2 ± 0.8 |
| | pH | 3.9 ± 0.1 | 3.9 ± 0.1 | 3.9 ± 0.02 | 3.9 ± 0.03 |
| Phase 4 | COD / (g L ⁻¹) | 3.0 ± 0.4 | 3.0 ± 0.4 | 3.0 ± 0.4 | 3.0 ± 0.4 |
| | pH | 6.2 ± 0.4 | 6.2 ± 0.4 | 6.2 ± 0.4 | 6.2 ± 0.4 |

HRT: hydraulic retention time; COD: chemical oxygen demand.

CTO-20A oven, an LC-10 ADVP pump, an SCL 10AVP control, an Aminex HPX-87H column (300 mm × 7.8 mm) (BioRad) and H₂SO₄ (0.01 M) at 0.5 mL min⁻¹ flow rate as eluent.¹¹

In addition to sugars measurement, total carbohydrates were analyzed by the phenol-sulfuric method.¹² The biogas production was measured using gas meters¹³ coupled to the headspace of the reactors. Biogas composition (H₂, CO₂, and CH₄) was evaluated using a gas chromatography set (model GC-2010, Shimadzu Scientific Instruments, Kyoto, Japan) equipped with a thermal conductivity detector (GC/TCD), argon as the carrier gas and Carboxen 1010 PLOT column (30 m × 0.53 mm).¹¹

Molecular microbiology

Total DNA was extracted at the end of the operational period using acid-washed glass beads (Sigma-Aldrich, St. Louis, MO, USA), followed by washing consecutively with phenol and chloroform.¹⁴ The metagenomic sequence and analysis were performed in duplicate using the total DNA extracted at the end of operation period of reactor 3 (R3). The library preparation and metagenomic sequencing were performed at MR DNA (www.mrdnab.com, Shallowater, TX, USA) following Illumina's guidelines. Briefly, 50 ng of DNA were used to prepare the libraries using the NextEra DNA sample preparation kit (Illumina, San Diego, CA, USA). The quality of the sequences was evaluated using the FastQC program.¹⁵ Trimmomatic tool¹⁶ was applied to filter reads with phred score ≤ 20.

Diamond alignment tool¹⁷ was used to align reads to the Kyoto Encyclopedia of Genes and Genomes (KEGG) database¹⁸ for functional annotation and, finally, GenBank NR database¹⁹ was used for taxonomic annotation with the lowest common ancestor (LCA) parameter. The Prodigal results were aligned with the carbohydrate-active enzymes database²⁰ using the Diamond tool with cutoff of >80% identity, e-value 1e-3, and coverage of 80%. The taxonomic annotation of open reading frames (ORF) aligned in the CAZY database was performed in the Kaiju tool²¹ using the GenBank NR database.¹⁹

The filtered reads were co-assembled using MegaHit²² of the SqueezeMeta tool²³ with 150 bp minimal length of contig and k-mer range of 21-119. Bowtie2²⁴ and Bedtools²⁵ mapped and counted the contigs, respectively. ORF calling and total protein sequence prediction were performed using Prodigal.²⁶ Sequencing reads were deposited in the European Nucleotide Archive under Project number PRJEB34240.

RESULTS AND DISCUSSION

Sugarcane bagasse and hydrolysate characterization

The main physicochemical characteristics of the raw pentose liquor included: COD = 175 g L⁻¹, total carbohydrates = 81.5 g L⁻¹, phenols = 28 g L⁻¹, total solids (TS) = 76.50 mg L⁻¹, total volatile solids (VS) = 157.25 mg L⁻¹ and pH = 3.4. The hydrothermal pretreated sugarcane bagasse was composed of cellulose (59.8%), hemicellulose (10.1%) and lignin (23.9%). The crystallinity index was 48%, while TS and VS were 0.94 and 0.82 g kg⁻¹ with 0.03% of moisture. The compositional analysis resulted in 66% of carbon, 18.9% of oxygen, and 7.4% of nitrogen. Different compositions have been reported for sugarcane bagasse. The untreated fiber used by Sá *et al.*,²⁷ consisted of 39.99 ± 3.50% of cellulose, 21.82 ± 4.43% of hemicellulose and 26.51 ± 1.45% of lignin, while the sugarcane bagasse used by Gonzalez-Leos *et al.*,²⁸ was formed by 34.47 ± 0.5% of cellulose, 29.73 ± 0.98% of hemicellulose and 35.4 ± 0.37% of lignin, indicating the importance of characterizing the material for improving the fermentation process.

The hydrothermal pretreatment breaks down the lignocellulosic structure, releasing fermentable sugars (mainly five-carbon molecules in the liquid fraction, that's why the term "pentose liquor") and facilitating access to the cellulolytic substrate for microorganisms. As a direct response to the hydrothermal pretreatment, the cellulose content increases, with the simultaneous reduction in lignin and xylan contents in the solid fraction. The partial degradation of xylan releases xylan oligomers, while the hydrophobic lignin and less reactive cellulose persist in the fiber¹ and can be used as substrate for fermentative energy production.

Overall performance of the innovative bioreactor: metabolite production

The mean influent pH in phases 1, 2, and 3 was 5.8 ± 0.3, 4.2 ± 0.2, and 4.0 ± 0.03, due to the low pH of the hydrolysate (pH 3.4 ± 0.1) used as substrate, once there was no alkalization of the systems. In contrast, sodium bicarbonate was used as an alkalizing agent in phase 4, which explains the higher pH (6.2 ± 0.3) compared to the former phases. According to Oliveira *et al.*,⁴ the usual pH of fermentative fixed-bed reactors producing hydrogen is 5.5; however, these authors reported continuous and stable hydrogen production at relatively unfavorable pH (3.8) using sugarcane molasses as substrate, *i.e.*, another carbohydrate-rich substrate. Carbohydrate removal showed increasing patterns in all reactors, rising from 15.2 to 68.4% in R1, 41.1 to 68.3% in R2, 48.1 to 63.7% in R3 and 22.3 to 65.6% in R4.

The mass balance (Figure 2) was based on the organic matter content (COD) and included the intermediate metabolites, the remaining (unconverted) carbohydrates and the recalcitrant fraction, which may include phenols and additional metabolites not considered in the analytical methods but released in the hydrothermal pretreatment of sugarcane bagasse. The distribution of the organic compounds varied considerably according to the operating phase, usually showing higher proportions of intermediate metabolites during the application of lower COD levels (mainly in R1 and R2; Figure 2). Meanwhile, the application of higher HRT levels (R1 and R2) were associated with the predominance of recalcitrant compounds (R1) or unconverted carbohydrates (R2) when the COD was increased to 9.0 g L⁻¹ (Figure 2). No specific distribution patterns were observed when applying lower HRT levels (R3 and R4), despite the increase in the fraction of unconverted carbohydrates in both systems as the COD was increased (Figure 2). No methane was produced in all the reactors, indicating the effectiveness of inoculum pretreatment and corroborating the negative effect of the acidic pH on the microbial communities, which suppressed the growth of methanogenic archaea.

In phase 1, a decreasing trend in the hydrogen fraction in biogas was observed when comparing reactors R1 (HRT = 56 h), R2 (42 h) and R3 (28 h), with the lowest and highest values observed in R1 (69.8 ± 22.3%) and R3 (95.2 ± 1.3%), respectively. The application of the lowest HRT (14 h, R4) resulted in a hydrogen fraction of 81.2 ± 16.2%, suggesting the occurrence of an optimal HRT near 28 h. Higher hydrogen proportions were also observed in the application of lower HRT, *i.e.*, 24.3% (HRT = 24 h) and 36.9% (HRT = 8 h) in the case of upflow anaerobic packed-bed reactors fed with sugarcane vinasse at 55 °C.²⁹ In phase 2, similar H₂ fractions were observed in R1 (88 ± 9.1%, HRT = 56 h), R2 (88.9 ± 5.2%, HRT = 42 h) and R4 (81.2 ± 6.4%, HRT = 14 h), while the highest percentage (93.2 ± 1.4%) was observed in R3 (HRT = 28 h). In phase 3, characterized by the highest COD (9.0 g L⁻¹), no H₂ production was observed in the reactors, regardless of the HRT, indicating that the microbial populations were severely affected by the applied COD and acidic pH. In phase 4, H₂ percentage was high and stable in all

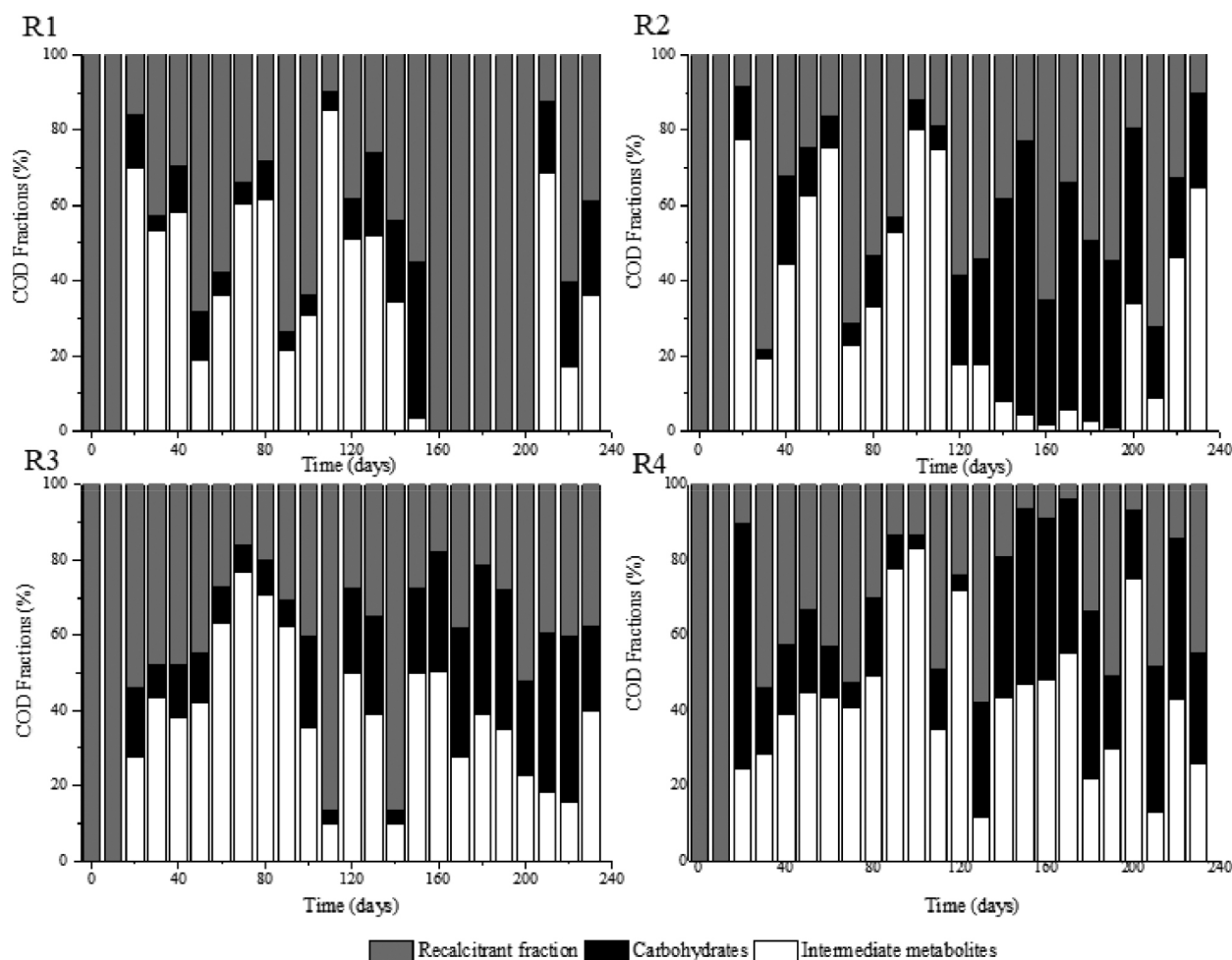


Figure 2. COD-based mass balance considering the soluble phase intermediate metabolites, carbohydrates and recalcitrant fraction

reactors ($84.3 \pm 4.3\%$, $90.0 \pm 2.2\%$, $91.3 \pm 3.7\%$ and $80.5 \pm 5.2\%$ in R1, R2, R3 and R4, respectively). The highest H_2 percentage in phase 4 was obtained when applying an HRT of 28 h in R3, which was also the reactor showing the highest H_2 percentages in phases 1 and 2 ($95.2 \pm 1.3\%$, and $93.2 \pm 1.4\%$, respectively), characterizing 28 h as the optimum HRT to obtain H_2 from SCB hydrolysate.

Although H_2 was detected in all reactors in phases 1, 2, and 4, the biogas flow rate was observed only in the last phase in reactors R2 and R3 (HRT of 42 h and 28 h, respectively). Maximum H_2 production of 66 mL (R2, HRT = 42 h) and 686 mL (R3, HRT = 28 h) shows the effect of the HRT on the metabolic pathways established during substrate fermentation. The mean hydrogen yield (HY) values were 0.22 and 1.63 mol H_2 mol⁻¹ carbohydrate in R2 and R3, respectively. Equivalent HY values (1.4-1.5 mol H_2 mol⁻¹ carbohydrate) were observed in sugarcane vinasse fermentation using thermophilic bench-scale fixed-bed reactors.^{29,30} Low HY is related to unfavorable conditions for the fermentation process, such as low substrate availability.³⁰ Excess substrate availability, which characterizes conditions of organic overloads, also impair the production of hydrogen by stimulating non- H_2 -producing (lactate production) and/or H_2 -consuming (propionate production) pathways. In addition to the potential occurrence of organic overloading conditions in phase 3, the relatively high proportion of recalcitrant compounds in the hydrolysate, such as phenols, may have been an additional inhibitory factor to hydrogen-producing bacteria.

Regarding the production of organic acids, reactors R1 and R4 (HRT of 56 h and 14 h, respectively) presented a similar profile (Figure 3), in which acetic acid prevailed in the first phase and lactic

acid accumulated in subsequent phases. The maximum theoretical HY (4 mol mol⁻¹ hexose) is associated with acetic acid production.^{31,32} Acetic acid can be produced from different pathways, namely, acidogenesis, acetogenesis, and homoacetogenesis. In the first pathway, fermentative bacteria convert carbohydrates into alcohols, H_2 , CO_2 , acetic and other fatty acids. Acetogenic bacteria oxidize organic acids and solvents to acetic acid, H_2 , and CO_2 , while homoacetogenic bacteria convert H_2 and CO_2 into acetic acid.^{31,32} Because hydrogen is consumed in the latter pathway, high acetic acid concentrations will not be necessarily associated with high hydrogen production levels.

Despite the high hydrogen production in biogas in R1 and R4 during phase 1, the null biogas flow rate indicates that acetic acid was mainly produced *via* the homoacetogenic pathway. The homoacetogenic activity can be estimated *via* mass balance according to the intermediate metabolites and hydrogen yield.³² In all phases of R1 (HRT = 56 h) homoacetogenesis was the main acetic acid-producing pathway, accounting for 80% of the total acetogenic activity in the last phase.

While applying phase 1 in R2, almost 93% of the total acetic acid was produced *via* homoacetogenesis. However, with the increase in the organic matter content in the subsequent phases, no acetic acid was produced, indicating that this metabolic pathway was inhibited under an HRT of 42 h most likely by the excess of organic matter (both readily available and recalcitrant fractions). In R3 (HRT = 28 h), the percentage of acetic acid produced *via* homoacetogenesis increased according to the organic matter content increase and reached 42.3% in phase 3. However, in phase 4, in which the highest hydrogen production was observed, this pathway was responsible for only 14.1% of the total produced acetic acid.

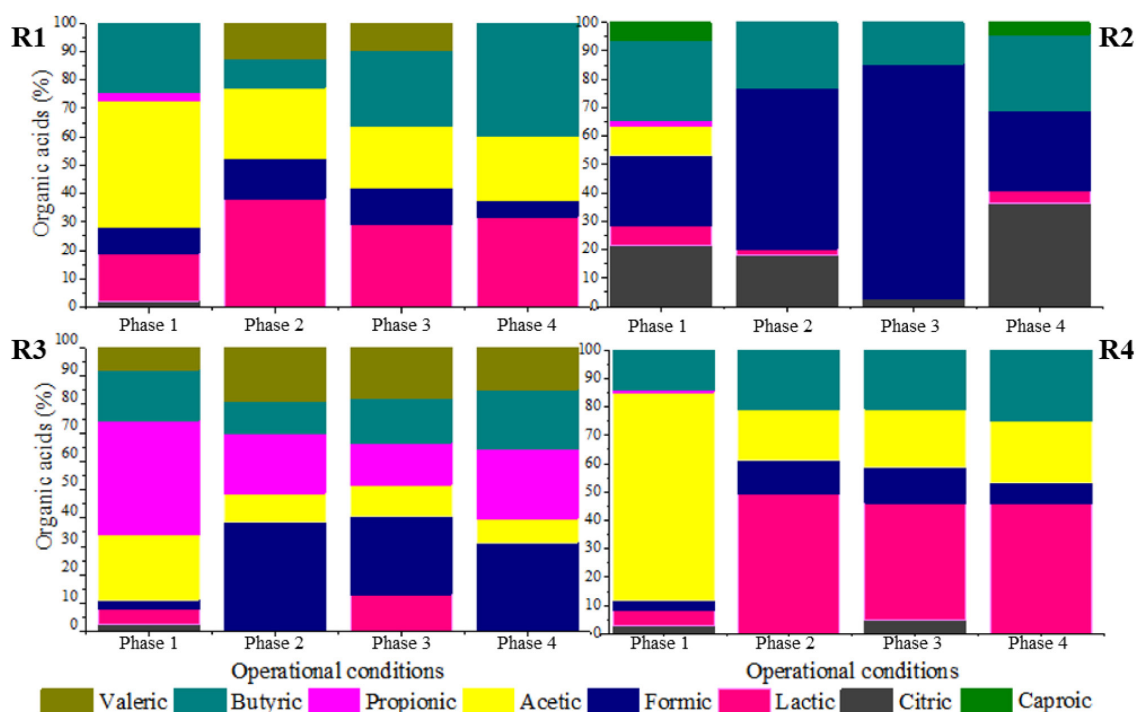


Figure 3. Distribution of organic acids at the different HRT of 56 h (R1), 42 h (R2), 28 h (R3), and 14 h (R4) according to the operational phases

Baima *et al.*,³¹ also reported an increase in the homoacetogenic activity as a function of the HRT reduction, *i.e.*, from 23 to 51% (HRT decrease from 24 to 2 h) followed by a subsequent decrease to 45% under an HRT of 1 h, using sugarcane molasses as the substrate in mesophilic expanded granular sludge bed reactors. In contrast, 64.5, 60.3, and 64.1% of the acetic acid quantified in phases 2, 3, and 4 in R4 were produced *via* homoacetogenesis, against 38.7% in phase 1. This pattern indicates that the lowest HRT (14 h) favored homoacetogenic bacteria, even at the lowest pH resulting from the increase in the organic matter content (due to the lower dilution level of the hydrolysate). These bacteria are obligate anaerobes that perform Wood-Ljungdahl as the primary pathway for energy conservation, cell carbon synthesis and for acetyl-CoA synthesis from CO₂, resulting in acetic acid production as the main intermediate metabolite.³³ Homoacetogenesis is a key-step in methanogenic systems by regulating the partial pressure of hydrogen in the reactors, but the process characterizes an unwanted pathway in hydrogen-producing reactors due to the consumption of hydrogen.

In R1 and R4, similar profiles were observed for lactic acid production, which was one of the main intermediate metabolites in phases 2, 3, and 4 under both HRT (56 and 14 h, respectively). Lactic acid bacteria (LAB) compete for substrates, mainly carbohydrates, with other fermenting bacteria, delaying or even eliminating the production of hydrogen. Besides lactic acid, due to the heterofermentative nature of some groups, LAB can produce other by-products, such as acetic acid and ethanol, while homofermentative LAB can outcompete the other strains in glucose consumption, leading to lactic acid accumulation.³⁴

More importantly, lactic acid production decreases the pH of the fermentation medium, generating a bacteriostatic or even bactericidal environment for many bacteria,³⁵ which was observed in R1 and R4. In addition, LAB also present many mechanisms such as biofilm generation, conjugation, competence, bacteriocin production, and pathogenesis as bacterial regulation, which plays a role in stress responses and inhibits the activity of other bacterial groups,³⁵ such as the *Clostridium* genus.

The proportion of lactic acid in R1 increased from 16.8% in phase 1 to 38.3% in phase 2, further decreasing to 29.2% in phase 3.

In phase 4, this metabolite accounted for 31.8% of the measured metabolites, close to that obtained in phase 2 in which similar organic matter contents were applied (3.2 ± 0.3 and 3.0 ± 0.4 g COD L⁻¹ in phases 2 and 4, respectively). However, the pH dropped from 6.3 ± 0.3 to 4.8 ± 0.2 in phase 4 in R1, corroborating the LAB ability to inhibit other bacteria by decreasing the pH and its tolerance to acidic stress. In R2 and R3, low lactic acid accumulation was observed in all operational phases. In R2, the highest lactic acid accumulation corresponded to 21.4% in phase 1, reaching 13.1% in phase 3 in R3. No lactic acid was observed in R3 in the last phase, and minimal lactic acid accumulation was observed in the same phase in R2 (4.4%), in which H₂ production was observed.

The highest lactic acid percentage was observed in R4, in which the lowest HRT was applied (14 h). In phase 1, 5.6% of the measured fermentation metabolites corresponded to lactic acid, a value that increased to 49.1% in phase 2. In phase 3 and 4, the lactic acid accumulation accounted for 41.2 and 45.8% of total metabolites, respectively, indicating that the low HRT was favorable to LAB populations. Ferreira *et al.*,³⁶ reported that it is likely that the decrease in the HRT from 6 to 1 h favored the increase in lactic acid production (from 11.7 to 33.1%) during the fermentation of sugarcane juice under thermophilic condition in an anaerobic fluidized-bed reactor (AFBR), corroborating the positive effect of low HRT in the performance of LAB.

Besides the similar patterns observed for acetic and lactic acid production in R1 and R4, the production of isovaleric acid in phases 2 and 3 (12.4 and 9.8%, respectively) in R1 was a marked difference between these reactors. It is important to highlight that isovaleric acid is produced mainly using hydrogen-consuming pathways,³³ such as *via* propionic acid bioconversion, which was corroborated by the production of propionic acid in the first phase and its complete consumption in the next phases, with concomitant isovaleric acid production in R1.

Isovaleric acid was also produced in R3 in all phases (7.7, 18.7, 18.0 and 14.7% in phase 1, 2, 3, and 4, respectively). Ca. 3.8 g L⁻¹ of isovaleric acid was produced in R3 during phase 3. Chain elongation towards isovaleric acid production could be a consequence of

propionic acid accumulation, which results in a competition for electron donors, such as ethanol or lactic acid.³⁷ The isovaleric acid accumulation reported in the present study is in line with previous studies showing significant amounts of isovaleric acid during sugarcane bagasse fermentation.³ However, although valeric acid has been widely produced in anaerobic reactor processing sugarcane-derived products,³¹ its pathway and role in fermentative processes is still unclear and underexplored.

In R3, the reactor showing the highest hydrogen production, propionic acid was the predominant acid in the first phase (40.3%), while in R1, R2 and R4 this metabolite corresponded to only 2.8, 1.9, and 0.9% of the total metabolites. In phase 2, propionic acid was produced only in R2 and R3 (3.4 and 3.0 g L⁻¹, respectively), while it was produced only in R3 (3.1 and 1.7 g L⁻¹ in phases 3 and 4, respectively) in the subsequent phases. Although hydrogen production was observed in R3, propionic acid production is a hydrogen-consuming pathway, negatively impacting hydrogen evolution.

Propionic acid can also be produced through lactic acid degradation,³⁰ a possible microbial pathway established in R3, once lactic acid was maintained at low levels in all operational phases of this reactor. In the subsequent phases, the distribution of metabolites suggests that propionic acid was converted into valeric acid, once the increase in the proportion of the latter was marked by the consumption of the former. The results obtained in this study indicate that propionic acid production was favored under an HRT of 28 h, because this metabolite accumulated in all phases assessed in R3, while some minor concentrations were obtained only during phase 1 in R1, R2, and R4. The high organic matter content and low pH were beneficial for the enrichment of propionate-producing bacteria in R3, as demonstrated by the high propionate concentrations (> 3.0 g L⁻¹) in phases 2 and 3, when COD levels of 3.2 ± 0.4 and 9.2 ± 0.7 g COD L⁻¹ and pH of 4.3 ± 0.2 and 3.9 ± 0.03 were applied. Meanwhile, the concentration of propionic acid dropped by the half (1.7 g L⁻¹) in phase 4, most likely as a direct result of the higher pH (6.2 ± 0.4), considering a lower interference of the COD (similar to phase 2).

According to Saady,³³ similar to LAB, propionate-producing bacteria are associated to stress condition, such as organic overloads, in which the propionic-type pathway acts as a hydrogen sink to alleviate the establishment of high hydrogen partial pressures resulting from the enhanced activity of hydrogen-producing bacteria. Low pH values (5.1-3.5) have been also demonstrated to be favorable for stable propionic acid production from sweet sorghum extract in a continuous stirred-tank bioreactor.³⁸

Formic acid production was another dominant metabolic pathway observed in R3, which prevailed in all phases assessed in R2, reaching 82% of the metabolites in phase 3. Formic acid production is an alternative to store hydrogen with zero CO₂ emission.³⁹ Therefore, in the present study, hydrogen was produced either from the reduced form of ferredoxin or through the decomposition of formic acid when acetyl-CoA is produced from pyruvic acid.³⁸

In R2, two other fermentation intermediates, namely, citric and caproic acids, also deserve attention: while citric acid production was observed throughout the entire operational period, caproic acid was produced only in phases 1 and 4. The anaerobic production of citric acid occurs *via* the incomplete reductive citric acid cycle pathway, which is essentially the oxidative citric acid cycle running in reverse.⁴⁰ The incomplete reductive citric acid cycle runs in reverse due to three key enzymes (ATP citrate lyase, 2-oxoglutarate:ferredoxin oxidoreductase, and fumarate reductase) which are involved in the cleavage of citrate to acetyl-CoA, carboxylation of succinyl-CoA to 2-oxoglutarate, and reduction of fumarate forming succinate.⁴⁰

Caproic acid can be produced during the fermentation using short chain carboxylic acids, such as acetic, butyric and lactic acids as

precursors.³⁷ According to the Gibbs free energy (ΔG), caproic acid production can be spontaneous as it yields more energy than butyrate formation. In this study, caproic acid production was accomplished by butyric acid reduction, indicating that this metabolite was preferably converted into caproate. Some complex substrates, such as sugarcane juice, can be successfully used for carboxylic acid chain elongation and caproic acid production,³⁷ corroborating its production from hydrolysate SCB in this study.

The production of organic acids was accompanied by variations in the concentration of sugars along the vertical profiles of the reactors. Figure 4 depicts specifically the vertical profiles obtained in phase 4 for all reactors. The spatial profiles of sugar concentrations demonstrate concomitantly their consumption and release by the microbial communities. In phase 4, sucrose, glucose, xylose, and arabinose (187.6, 211.6, 368.4, and 61.6 mg L⁻¹, respectively) were observed in the hydrolysate used to feed the reactors. Sucrose is the dominant form of nonstructural carbohydrate in the sugarcane and it is one of the constituents of sugarcane juice used for ethanol production.⁴¹ On the other hand, arabinose and galactose are released from hemicellulose, while glucose can be produced from both cellulose and hemicellulose.⁴²

In R1, 99% of the total sugars were converted in the first compartment (L/D = 0.3). After the first solid compartment (L/D = 1.5), sucrose and xylose were released, indicating fiber degradation by microorganisms adhered to SCB fibers. In R2, sugar concentrations showed an increasing pattern along the vertical profile, with galactose reaching 300 mg L⁻¹ in the last compartment (L/D = 6.3), indicating hemicellulose degradation. In contrast, no increase in sugar concentrations was observed in R4 (from L/D = 0.3 to L/D = 5.1) indicating the simultaneous release and conversion of sugars. The release of sucrose, xylose and traces of glucose in the last compartment (L/D = 6.3) of R4 corroborates the occurrence of SCB degradation. In R3, the non-observation of galactose, the complete conversion of glucose and the detection of traces of xylose from L/D = 3.9 upwards indicate the preferential consumption of hexoses, resulting in the highest hydrogen production level (686 mL) observed among all reactors.

The production of hydrogen from pentoses or hexoses is characterized as acetic/butyric-type fermentation (Equations 1-4).²⁷ The preferential consumption of hexoses prior to pentoses was previously reported by Rabelo *et al.*,⁴³ as a response of a regulatory process called carbon catabolite repression (CCR), which prevents the consumption of secondary carbon sources before the preferential carbohydrates are utilized.⁴⁴ This regulatory mechanism prevents the uptake of non-preferred sugars before the consumption of preferred carbohydrates,⁴⁵ which most likely delayed the consumption of xylose before the complete uptake of galactose and glucose in R3.



The release of sugars through the degradation of the solid fraction in the reactors throughout the operation resulted in the decrease of the solid content in each compartment. At the beginning of the operation, each fiber-containing compartment was filled with 1 g of hydrothermally pretreated SCB, which was approximately reduced by the half on the course of the continuous fermentation (Figure 5). This corroborates the potential of the innovative compartmentalized

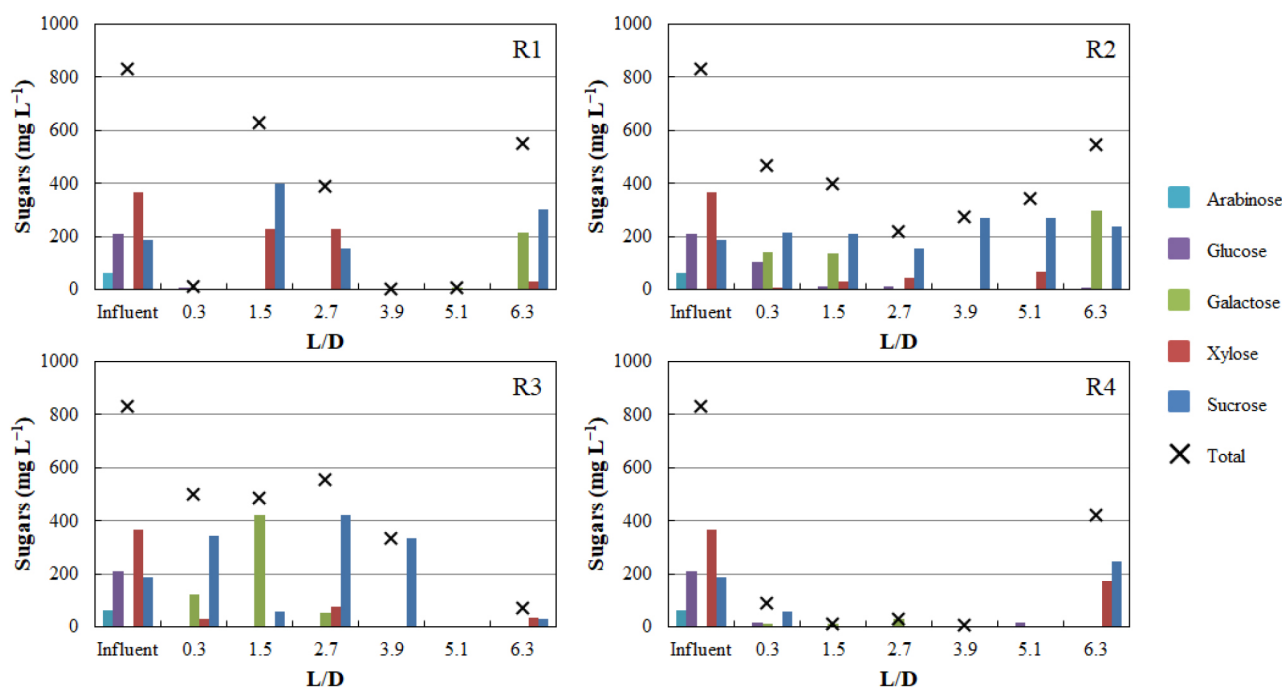


Figure 4. Sugar concentrations along the vertical profile of all the reactors in phase 4

reactors for recovering metabolic products concomitantly from both the hydrolysate and fibers, in addition to degrading the latter.

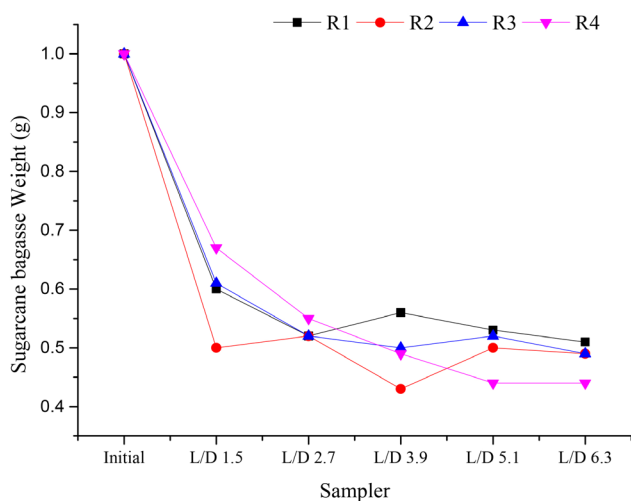


Figure 5. Sugarcane bagasse weight along the vertical profile of the reactors at the end of the operation

Structural, taxonomic and functional metagenomic profile of the microbial communities

The morphological analysis of SCB before and after the operation by scanning electron microscopy (data not shown) revealed microbial biomass attachment to the fibers in all reactors, corroborating the use of the fibers as support material for biofilm formation. Due to the superior hydrogen production associated to R3, only the microbial biomass sample collected from this reactor in phase 4 was subjected to metagenomic sequencing and analysis. Figure 6 displays the taxonomies of the microbial community in this sample. To assess the potential enzymes (Figure 6b) involved in the assembly (glycosyltransferase) and breakdown of carbohydrates (glycoside hydrolase, polysaccharide lyases, carbohydrate esterases) in R3, the carbohydrate-active enzyme (CAZy) genes database was accessed (<http://www.cazy.org/>).²⁰

Approximately 99.99% of the microbial communities found in R3 were associated to the bacteria domain, which was expected once no methane was observed in this reactor. At the phylum level, Firmicutes (67.7%) prevailed in R3, followed by Proteobacteria (29.45%).

Many different aerobic bacteria, in nature, degrade lignin-derived aromatic compounds, but the bioconversion of the latter under anaerobic condition has not been well investigated. Andreoni *et al.*,⁴⁶ reported that the genus *Pseudomonas* was able to metabolize ferulic acid, one of the simplest model compounds found in lignin, under anaerobic conditions. In this study, *Pseudomonas* was the second most abundant genus (21.08%) in R3, and was probably a key microorganism in lignin degradation. The most dominant enzymes (relative abundance higher than 1%) involved in the decomposition of recalcitrant lignocellulosic biomass or modifying carbohydrates from the group of glycoside hydrolases (GHs) are presented in Figure 6b.

Under anaerobic conditions, lignin degradation requires many different microbial enzymes to cleave specific bonds according to its crystallization. As lignin is the most abundant aromatic polymer (phenolic), its degradation involves anaerobic phenol bioconversion into non-aromatic compounds. This process is performed in many steps by bacterial enzymes such as phenylphosphate synthase (K01007), phenylphosphate carboxylase (K03182), AMP-forming carboxylic acid coenzyme A ligase (K01895), benzoyl-CoA reductase subunit A (K04114) and subunit D (K04115),⁴⁷ all of them identified in the present study (0.12, 0.01, 0.03, 0.01, and 0.006%, respectively), supporting lignin degradation.

In the same way, *Clostridium* genus includes numerous highly active anaerobic cell wall degraders, with many species associated to thermophilic hemicellulolytic metabolism.² *Clostridium* was the most abundant genus in R3 (44.23%) and includes strictly anaerobic bacteria with high potential for bioenergy production from numerous organic substrates via one and/or two-step conversion. In the direct fermentation, cellulolytic enzymes are responsible for the one-step degradation of lignocellulosic biomass, while separated hydrolysis and fermentation occur in the two-step bioconversion.⁴⁸

Bacillus is another cellulolytic genus identified in R3 (1.36%), characterized by the production of CMCase, cellulases and xylanases and, therefore, being able to degrade celluloses and hemicelluloses.⁴⁹

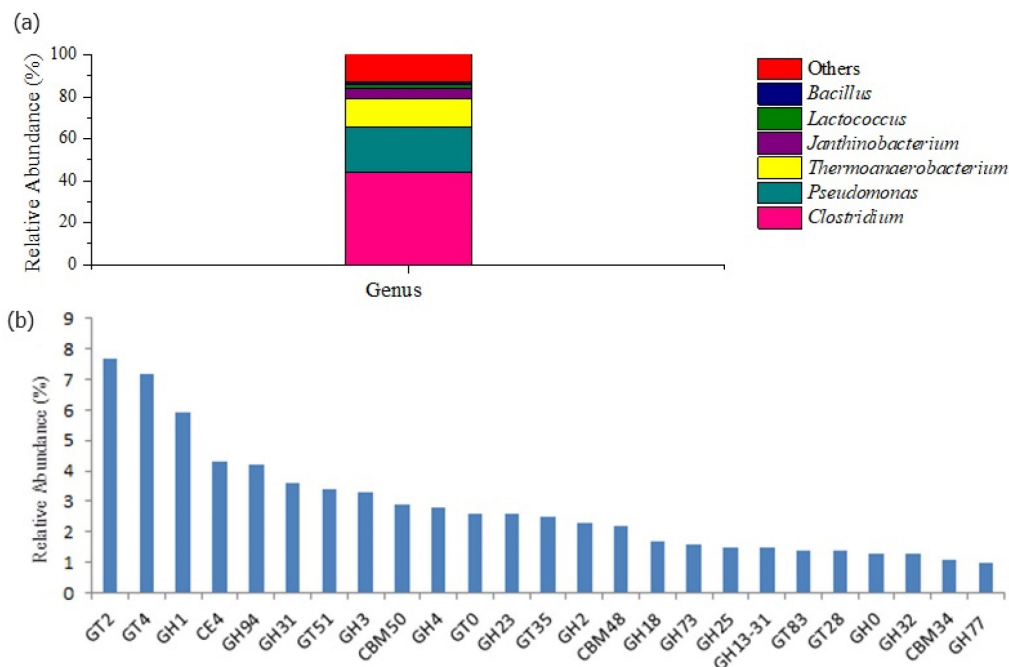


Figure 6. Microbial taxonomy (a) and enzymatic profile (b) in R3 according to the relative abundance: GT2 and GT4 (7.7 and 7.2%, respectively) followed by GH1 (5.9%), CE4 (4.3%), GH94 (4.2%), GH31 (3.6%), GT51 (3.4%), GH3 (3.3%), CBM50 (2.9%), GH4 (2.8%), GT0 (2.6%), GH23 (2.6%), GT35 (2.5%), GH2 (2.3%), CBM48 (2.2%), GH18 (1.7%), GH73 (1.6%), GH25 (1.5%), GH13-31 (1.5%), GT83 (1.4%), GT28 (1.4%), GH0 (1.3%), GH32 (1.3%), CBM34 (1.1%), GH77 (1.0%)

This genus also plays an important role in dye decolorization under anaerobic conditions.⁵⁰ In the same way, LAB from the genus *Lactococcus* were associated to azo dye reactive black 5 and anthraquinone dye remazol brilliant blue R degradation under hydrolytic-fermentative condition.⁵⁰ Therefore, *Bacillus* (1.36%) as well as *Lactococcus* (2.2%) may have played an important role in the removal of color from the dark SCB hydrolysate used as liquid substrate in this study.

The enzymes from the group of glycoside hydrolases (GHs) include cellulases and hemicellulases, widely required for the bioconversion of lignocellulosic biomass into oligo- and monomeric compounds. According to the substrate specificities, cellulases are grouped in the class of (i) endoglucanases, which are able to hydrolyze the amorphous region of cellulase to release oligosaccharides, cellobiose and glucose; (ii) cellobiohydrolases, also called exoglucanases, which release cellobiose from the reducing and non-reducing ends of cellulose; and, (iii) β -glucosidases, which are able to convert cellobiose and short oligosaccharides into glucose.⁵¹ Similarly, the carbohydrate binding modules (CBMs) is an associated modular structure related to the adhesion of microorganisms to the carbohydrates.⁵² Therefore, in the hydrolysis step, the main constituents of hydrolysate and SCB fibers (cellulose, hemicellulose and lignin) were bioconverted into soluble monomeric compounds, such as sugars, fatty acids, and non-aromatic compounds by hydrolytic bacteria, such as *Pseudomonas*, *Clostridium* and *Bacillus*.

Subsequently, the simple compounds released during hydrolysis were converted into organic acids and hydrogen by fermentative bacteria. The genus *Janthinobacterium*, which is associated to the degradation of structural polysaccharides for hydrogen production in mature hydrogen-producing granules from UASB reactor,⁵³ was observed in R3 (4.46%). This genus also performs an important role in co-oxidation of complex compounds such as toluene, xylene, naphthalene, and benzene.⁵⁴

The genus *Thermoanaerobacterium*, widely studied as ethanol-producing bacteria, is also able to produce organic acids and hydrogen.

Saripan and Reungsang,⁵⁵ reported 55 °C as the optimal temperature for hydrogen production from xylose by *Thermoanaerobacterium* via acetate-type fermentation. The genus *Thermoanaerobacterium* was selected and favored in the present study (14.12%) under thermophilic condition (55 °C), and can be associated to the production of hydrogen, acetic and butyric acids in R3. In agreement with this study, the genus *Thermoanaerobacterium* has been reported as an important moderate thermophilic hydrogen-producer from sugarcane by-products such as vinasse³⁰ and molasses.⁴

The bioconversion of vinasse³⁰ and lignocellulosic biomass, such as filter paper⁴⁸ and sugarcane bagasse² into hydrogen is also associated to bacteria belonging to the genus *Clostridium*. This genus is also able to produce formic acid from pyruvate and coenzyme-A by means of an essential enzyme in bacterial anaerobic metabolism, pyruvate formate lyase (K04069).⁶ In the present study, this enzyme was identified in relative abundance of $0.06 \pm 0.0006\%$, suggesting this pathway was most likely responsible for formic acid production in the reactors. In addition, the genus *Clostridium* is able to convert lactic acid into propionic acid via propanoate metabolism (Keeg_ec00640).⁵⁶ The first step of this pathway is performed by the lactyl CoA enzyme (K01026), which was identified in R3 ($0.03 \pm 0.001\%$) and most likely actively participated in propionic acid production. This explains the non-detection of lactic acid in this reactor in the last operating phase.

In the same way, species of *Clostridium*, such as *C. kluyveri*, can ferment propionic acid to valerate,⁵⁷ which accounted for 14.7% of the metabolites produced in R3 during phase 4. In addition to these acids, butyric acid was also produced in R3 (21.1%) via acidogenesis. According to Liu *et al.*,⁵⁸ this intermediate can be produced as a result of syntrophic association between the genera *Thermoanaerobacterium* and *Clostridium*. Therefore, the genera *Thermoanaerobacterium*, *Janthinobacterium*, and *Clostridium* played key roles in substrate fermentation towards hydrogen and organic acids in R3.

Regarding acetic acid production, ca. 14% of the total acetic acid

was produced *via* homoacetogenesis in R3 (phase 4). Homoacetogenic bacteria shift their metabolism under stress conditions or after the depletion of the reduced organic substrate.³³ In this study, acetate-forming bacteria, such as the genus *Clostridium* probably performed the homoacetogenic metabolism as a result of the HRT, COD, and pH.

The original content of this manuscript can be found in the preprint version.⁵⁹

CONCLUSIONS

The operating conditions stimulated the production of hydrogen and soluble metabolites at different levels. Hydrogen production reached 1.63 mol H₂ mol⁻¹ carbohydrate when applying an HRT of 28 h, condition in which formic acid prevailed as the main soluble metabolite. Meanwhile, butyric, citric, and lactic pathways were favored at HRT of 56, 42, and 14 h, respectively. From a metagenomic point of view, *Clostridium* was the predominant genus (44.2%) with a potential participation in formic, valeric, and propionic metabolic pathways. Enzymes involved in the assembly (glycosyltransferase) and carbohydrates breakdown (glycoside hydrolase, polysaccharide lyases, and carbohydrate esterases) were found in high abundance, indicating a potential role in the degradation of sugarcane bagasse. Overall, the novel compartmentalized reactors presented potential to simultaneously maintain the hydrolysis of the solid fraction and the fermentation of the soluble fraction of sugarcane bagasse, which opens up possibilities to exploit this configuration in the processing of different combinations of solid and liquid residual substrates, such as bagasse + vinasse or other sugarcane-derived by-products.

ACKNOWLEDGMENTS

This work was supported by the Coordenação de Aperfeiçoamento de Pessoal de Nível Superior - Brasil (CAPES), finance code 001 and the Fundação de Amparo à Pesquisa do Estado de São Paulo (grant numbers 2017/07194-6 and 2015/06246-7). The authors would like to thank the Laboratório Nacional de Biorrenováveis (LNBR) for providing the sugarcane bagasse and the hydrolysate used in this study, as well as the Usina São Martinho for providing the thermophilic inoculum.

REFERENCES

- da Cruz, S. H.; Nichols, N. N.; Dien, B. S.; Saha, B. C.; Cotta, M. A.; *J. Ind. Microbiol. Biotechnol.* **2012**, *39*, 439. [Crossref]
- Soares, L. A.; Rabelo, C. A. B. S.; Delforno, T. P.; Silva, E. L.; Varesche, M. B. A.; *Renewable Energy* **2019**, *140*, 852. [Crossref]
- Ribeiro, F. R.; Passos, F.; Baeta, B. E. L.; Aquino, S. F.; *Sci. Total Environ.* **2017**, *584-585*, 1108. [Crossref]
- Oliveira, C. A.; Fuess, L. T.; Soares, L. A.; Damianovic, M. H. R. Z.; *Int. J. Hydrogen Energy* **2020**, *45*, 4182. [Crossref]
- Bayer, E. A.; Shimon, L. J. W.; Shoham, Y.; Lamed, R.; *J. Struct. Biol.* **1998**, *124*, 221. [Crossref]
- Cho, D. H.; Shin, S. J.; Kim, Y. H.; *Biotechnol. Bioprocess Eng.* **2012**, *17*, 270. [Crossref]
- Kim, S. H.; Han, S. K.; Shin, H. S.; *Process Biochem.* **2006**, *41*, 199. [Crossref]
- Atlas, R. M.; *Handbook of Media for Environmental Microbiology*, 2nd ed.; CRC Press: Boca Raton, 2005. [Crossref]
- Soares, L. A.; Braga, J. K.; Motteran, F.; Sakamoto, I. K.; Silva, E. L.; Varesche, M. B. A.; *Water Sci. Technol.* **2017**, *75*, 95. [Crossref]
- APHA; *Standard Methods for the Examination of Water and Wastewater*, 22nd ed.; Baird, R. B.; Eaton, A. D.; Clesceri, L. S.; Rice, E. W., eds.; American Water Works Association: Washington, 2017.
- Penteado, E. D.; Lazaro, C. Z.; Sakamoto, I. K.; Zaiat, M.; *Int. J. Hydrogen Energy* **2013**, *38*, 6137. [Crossref]
- Dubois, M.; Gilles, K. A.; Hamilton, J. K.; Rebers, P. A.; Smith, F.; *Anal. Chem.* **1956**, *28*, 350. [Crossref]
- Veiga, M. C.; Soto, M.; Méndez, R.; Lema, J. M.; *Water Res.* **1990**, *24*, 1551. [Crossref]
- Griffiths, R. I.; Whiteley, A. S.; O'Donnell, A. G.; Bailey, M. J.; *Appl. Environ. Microbiol.* **2000**, *66*, 1. [Crossref]
- Babraham Bioinformatics, <http://www.bioinformatics.babraham.ac.uk/projects/fastqc/>, accessed in February 2024.
- Bolger, A. M.; Lohse, M.; Usadel, B.; *Bioinformatics* **2014**, *30*, 2114. [Crossref]
- Buchfink, B.; Xie, C.; Huson, D. H.; *Nat. Methods* **2015**, *12*, 56. [Crossref]
- Kanehisa, M.; Goto, S.; Kawashima, S.; Nakaya, A.; *Nucleic Acids Res.* **2002**, *30*, 42. [Crossref]
- Benson, D. A.; Karsch-Mizrachi, I.; Clark, K.; Lipman, D. J.; Ostell, J.; Sayers, E. W.; *Nucleic Acids Res.* **2012**, *40*, D48. [Crossref]
- Lombard, V.; Ramulu, H. G.; Drula, E.; Coutinho, P. M.; Henrissat, B.; *Nucleic Acids Res.* **2014**, *42*, 490. [Crossref]
- Menzel, P.; Ng, K. L.; Krogh, A.; *Nat. Commun.* **2016**, *7*, 11257. [Crossref]
- Li, D.; Liu, C. M.; Luo, R.; Sadakane, K.; Lam, T. W.; *Bioinformatics* **2015**, *31*, 1674. [Crossref]
- Tamames, J.; Puente-Sánchez, F.; *Front. Microbiol.* **2019**, *9*, 3349. [Crossref]
- Langmead, B.; Salzberg, S. L.; *Nat. Methods* **2012**, *9*, 357. [Crossref]
- Quinlan, A. R.; Hall, I. M.; *Bioinformatics* **2010**, *26*, 841. [Crossref]
- Hyatt, D.; Chen, G. L.; LoCascio, P. F.; Land, M. L.; Larimer, F. W.; Hauser, L. J.; *BMC Bioinf.* **2010**, *11*, 119. [Crossref]
- Sá, L. R. V.; Faber, M. O.; Silva, A. S. A.; Cammarota, M. C.; Ferreira-Leitão, V. S.; *Renewable Energy* **2020**, *146*, 2408. [Crossref]
- Gonzalez-Leos, A.; Butos-Vásquez, M. G.; Rodríguez-Castillejos, G. C.; Rodríguez-Durán, L. V.; Del-Ángel, A.; *Rev. Mex. Ing. Quim.* **2020**, *19*, 377. [Crossref]
- Ferraz Júnior, A. D. N.; Wenzel, J.; Etchebehere, C.; Zaiat, M.; *Int. J. Hydrogen Energy* **2014**, *39*, 16852. [Crossref]
- Fuess, L. T.; Ferraz Júnior, A. D. N.; Machado, C. B.; Zaiat, M.; *Bioresour. Technol.* **2018**, *247*, 426. [Crossref]
- Baima, I. F. F.; Menezes, C. A.; Silva, E. L.; *Fuel* **2020**, *260*, 116419. [Crossref]
- Menezes, C. A.; Silva, E. L.; *Ind. Crops Prod.* **2019**, *138*, 111586. [Crossref]
- Saady, N. M. C.; *Int. J. Hydrogen Energy* **2013**, *38*, 13172. [Crossref]
- Eş, I.; Mousavi Khaneghah, A.; Barba, F. J.; Saraiva, J. A.; Sant'Ana, A. S.; Hashemi, S. M. B.; *Food Res. Int.* **2018**, *107*, 763. [Crossref]
- Papadimitriou, K.; Alegría, A.; Bron, P. A.; de Angelis, M.; Gobbetti, M.; Kleerebezem, M.; Lemos, J. A.; Linares, D. M.; Ross, P.; Stanton, C.; Turrone, F.; van Sinderen, D.; Varmanen, P.; Ventura, M.; Zúñiga, M.; Tsakalidou, E.; Kok, J.; *Microbiol. Mol. Biol. Rev.* **2016**, *80*, 837. [Crossref]
- Ferreira, T. B.; Rego, G. C.; Ramos, L. R.; Menezes, C. A.; Soares L. A.; Sakamoto, I. K.; Varesche, M. B. A.; Silva, E. L.; *Int. J. Hydrogen Energy* **2019**, *44*, 19719. [Crossref]
- Cavalcante, W. A.; Leitão, R. C.; Gehring, T. A.; Angenent, L. T.; Santaella, S. T.; *Process Biochem.* **2017**, *54*, 106. [Crossref]
- Antonopoulou, G.; Gavala, H. N.; Skiadas, I. V.; Lyberatos, G.; *Int. J. Hydrogen Energy* **2010**, *35*, 1921. [Crossref]
- Joó, F.; *ChemSusChem* **2008**, *1*, 805. [Crossref]
- Hügler, M.; Wirsén, C. O.; Fuchs, G.; Taylor, C. D.; Sievert, S. M.; *J. Bacteriol.* **2005**, *187*, 3020. [Crossref]
- Zhao, D.; Momotaz, A.; LaBorde, C.; Irely, M.; *Sugar Tech* **2020**, *22*, 630. [Crossref]

42. Phaiboonsilpa, N.; Chysirichote, T.; Champreda, V.; Laosiripojana, N.; *Energy Reports* **2020**, *6*, 710. [Crossref]
43. Rabelo, C. A. B. S.; Soares, L. A.; Sakamoto, I. K.; Silva, E. L.; Varesche, M. B. A.; *J. Environ. Manage.* **2018**, *223*, 952. [Crossref]
44. Stülke, J.; Hillen, W.; *Curr. Opin. Microbiol.* **1999**, *2*, 195. [Crossref]
45. Kim, J. H.; Block, D. E.; Mills, D. A.; *Appl. Microbiol. Biotechnol.* **2010**, *88*, 1077. [Crossref]
46. Andreoni, V.; Galli, E.; Galliani, G.; *Syst. Appl. Microbiol.* **1984**, *5*, 299. [Crossref]
47. Li, J.; Yuan, H.; Yang, J.; *Front. Biol. (Beijing, China)* **2009**, *4*, 29. [Crossref]
48. Lo, Y. C.; Huang, C. Y.; Cheng, C. L.; Lin, C. Y.; Chang, J. S.; *Bioresour. Technol.* **2011**, *102*, 8384. [Crossref]
49. Wu, Y.; Guo, H.; Zhang, J.; Chen, X.; Wu, M.; Qin, W.; *Waste Biomass Valorization* **2019**, *10*, 2517. [Crossref]
50. Xie, X.; Liu, N.; Yang, B.; Yu, C.; Zhang, Q.; Zheng, X.; Xu, L.; Li, R.; Liu, J.; *Int. Biodeterior. Biodegrad.* **2016**, *111*, 14. [Crossref]
51. Klippel, B.; Blank, S.; Janzer, V. A.; Piascheck, H.; Moccand, C.; Bel-Rhliid, R.; Antranikian, G.; *Extremophiles* **2019**, *23*, 479. [Crossref]
52. Bohra, V.; Tikariha, H.; Dafale, N. A.; *Appl. Biochem. Biotechnol.* **2019**, *187*, 266. [Crossref]
53. Ning, Y. Y.; Wang, S. F.; Jin, D. W.; Harada, H.; Shi, X. Y.; *Renewable Energy* **2013**, *53*, 12. [Crossref]
54. Tsavkelova, E. A.; Netrusov, A. I.; *Appl. Biochem. Microbiol.* **2012**, *48*, 421. [Crossref]
55. Saripan, A. F.; Reungsang, A.; *Int. J. Hydrogen Energy* **2013**, *38*, 6167. [Crossref]
56. Ohnishi, A.; Hasegawa, Y.; Abe, S.; Bando, Y.; Fujimoto, N.; Suzuki, M.; *RSC Adv.* **2012**, *2*, 8332. [Crossref]
57. Ding, H. B.; Tan, G. Y. A.; Wang, J. Y.; *Bioresour. Technol.* **2010**, *101*, 9550. [Crossref]
58. Liu, Y.; Yu, P.; Song, X.; Qu, Y.; *Int. J. Hydrogen Energy* **2008**, *33*, 2927. [Crossref]
59. Soares, L. A.; Delforno, T. P.; Oliveira, V. M.; Silva, E. L.; Varesche, M. B. A.; Fuess, L. T.; *Research Square*, 2023. [Link] accessed in February 2024